

A Review of Experimental Research on Hot Tearing of Aluminium Alloy Casting

Danyang Wang¹ · Liang Bai¹  · Wu Chen¹ · Hongxu Chang¹ · Jingshun Liu¹ · Ze Li¹

Received: 20 July 2023 / Accepted: 9 October 2023 / Published online: 21 November 2023
© The Indian Institute of Metals - IIM 2023

Abstract Since the 1950s, hot tearing has been extensively studied as a defect that severely affects the castability of aluminium alloy. However, mature commercial equipment that can characterize or test hot tearing formation has not yet been made, and the academic community have endeavoured to develop their own experimental methods to create hot tearing test systems. While there is no systematic review on hot tearing test system in this field, this paper provides a comprehensive review of recent research and experimental studies on testing systems for hot tearing in aluminium alloy casting with three focuses: (i) the research concept and initiation mechanism of hot tearing; (ii) experimental methods for studying hot tearing, including high-temperature tensile test deformation experiments, alloy-constrained solidification experiments and solidification tensile experiments; (iii) outlook on the development trends of various experimental equipments used to study hot tearing as well as research directions in this field.

Keywords Aluminium alloy · Casting · Hot tearing · Experiment · Test system

1 Introduction

In the process of alloy casting, common defects include shrinkage porosity, sand holes, cracks and other casting imperfections. Among them, hot tearing is one of the most prevalent issues in foundry production. If a hot tearing crack

occurs in an alloy during casting, its strength will be compromised and the cracks will be easily torn and expanded by stressors, which will significantly impact its practicality.

It is commonly accepted in the academic world that hot tearing arises from changes in the alloy's strength during its semi-solid state, which results in cracking. In 1914, Norton conducted experiments to evaluate the strength of semi-solid alloys by subjecting them to different weights. Since the 1950s, Bishop et al. have periodically conducted X-ray inspections on castings during solidification and concluded that alloys undergo hot tearing at the end of metal solidification above the solid phase line temperature (5–15 °C) [1, 2]. Therefore, many researchers have focused their studies on what happens to semi-solid alloy within this temperature range to cause cracking. After extensive research, four theories have been developed to explain the phenomenon of hot tearing in alloys: the liquid film theory [3, 4], the intergranular bridging theory [5], the strength theory and the solidification shrinkage compensation theory [6]. Despite the challenges posed by the sporadic hot cracking at high temperature, it is critical to understand its origin and development. Researchers have conducted a series of studies on the measurement and evaluation of hot tearing using various methods and have drawn many meaningful conclusions. However, due to the lack of a universally recognized quantitative standard for hot tearing testing, its testing and evaluation is still in the developmental stage [7, 8]. Research on the mechanism of hot tearing in alloys is ongoing with the continuous advancement in hot tearing testing methods. This paper focuses on experimental research of the formation of hot tearing in the casting process of aluminium alloy and summarizes the evolution, current status and future development direction of experimental testing methods in this process.

✉ Liang Bai
bailiang410@163.com

¹ Inner Mongolia University of Technology (IMUT), Hohhot, China

2 Experimental Measurements of Hot Tearing

Test methods for hot tearing have evolved from the high-temperature tensile test, which solely examines the tensile properties of an alloy at elevated temperatures, to experimental techniques involving constrained solidification and stochastic generation of hot tearing, and ultimately to research methods incorporating actively inducing hot tearing during alloy solidification. At present, most hot tearing testing methodologies are based on strength theory. Hot tearing occurs in the alloy when the solidification shrinkage stress exceeds or equals to the dendrites tensile strength during solidification process. The enlargement of thermal cracks is usually attributed to the shrinkage pores and other casting defects during alloy solidification caused by non-uniform solidification temperatures being subjected to solidification shrinkage stresses. This results in gradual expansion of shrinkage pores and initiation of thermal cracks along grain boundaries [9]. This chapter outlines research methods such as the high-temperature tensile test, alloy-constrained solidification experiment and solidification tensile experiment.

2.1 High-Temperature Tensile Test

It is widely recognized that hot tearing in alloys occurs during the late solidification stage; therefore, it is necessary to heat the alloy up to a specific temperature on the solid phase line prior to conducting tensile deformation experiments to measure the material strength at this temperature. According to the strength theory, hot tearing occurs when the solidification shrinkage stress of an alloy exceeds its tensile strength [10–13]. Therefore, precise measurement of high-temperature strength limit is crucial for predicting and identifying hot tearing [14, 15]. However, at elevated temperatures where strength is significantly reduced, maintaining the integrity of the semi-solid region becomes unattainable for alloys. Therefore, conventional tensile testing methods are inadequate and there is an urgent need to develop a high-temperature tensile testing apparatus capable of determining strength limits of alloys.

The traditional Instron® tensile tester has been improved to heat metals above the solid phase line. The improved Instron® tensile testing machine utilizes resistance heat as a heating method, wherein the tensile specimen held by a fixture is controlled on an upgraded resistance furnace, heated to the desired test temperature, and held at this temperature for a certain duration before conducting the tensile experiment. This approach enables accurate measurement of alloy strength limits at elevated temperatures. However, there are still some issues with this experiment. The utilization of a resistance furnace leads to prolonged heating time, resulting in phase transition within the alloy and inaccurate measurement of tensile stress. In addition, the strength of the alloy

significantly decreases due to the testing temperature reaching the solid–liquid two-phase zone, which cannot maintain its structural integrity. Consequently, the alloy deforms under gravity and shear stress is generated.

To address these issues, Han et al. [16] designed a novel reheating tensile testing method to evaluate the mechanical properties of the non-equilibrium paste region in 3004 alloy employing an Instron® 4507 tensile tester. The sample is first heated from room temperature to a temperature right above the solid phase line near the liquidus (620 °C and 630 °C) and then gradually cooled to the desired test temperature (600 °C). The alloy is then subjected to a specific temperature for a period of time in order to conduct the tensile test. Compared to the actual casting cooling process, this method ensures that the alloy has a consistent grain size and enhances accuracy of measuring the tensile stress limit.

In situ solidification can effectively address these issues by first heating the alloy to complete liquefaction, followed by gradual cooling it to the desired test temperature stretching it after a specific holding period. Subroto et al. [17] evaluated the semi-solid tensile mechanical properties of cast 7050 alloy using an Instron® 5944 tensile tester. To minimize the discrepancies in test results caused by experimental errors due to liquid metal adhering to the quartz tube, a boron nitride aerosol was coated on the surface of the quartz glass tube to reduce friction resistance. Additionally, this tensile testing equipment was utilized to investigate both semi-solid constitutive parameters and failure behaviour of cast AA7050 alloy.

The Gleeble® thermal simulation tensile test machine is also able to address these issues, which uses a Joule heat heating method that allows the alloy to be rapidly heated to the desired temperature, which can be maintained throughout the duration of the tensile test. This ensures a more accurate measurement of the tensile stress limit [18–20]. It can also perform in situ solidification experiments. In a study by Qing-ling Bai et al. [21], the alloy inside a quartz tube was heated up to its liquidus temperature and held for 60 s using A Gleeble® 3500 tensile test machine, then cooled down to the desired test temperature at a rate of 2 °C/s. Subsequently, the mechanical and constitutive properties of 7050 aluminium alloy were measured at the specified testing temperature.

However, in Gleeble® experiment, thermocouples are usually attached to the surface of the heated region of the sample by welding in order to regulate the heating temperature [13]. In high-temperature experiments, the solder joint of the thermocouple tend to detach, resulting in a low success rate of the experiment. There are three solutions to this particular problem of thermocouple connection. The first approach is to use the buried wire method, where two small holes are made on the sample's surface, into which the positive and negative thermocouple wires are inserted and fix it

[15]. However, this method is a destructive stationary technique that can result in inaccurate test data for mechanical properties. The second method involves wrapping the heated area of the sample with a metal mesh and welding a thermocouple to it to measure the temperature via heat conduction. This technique allows standard Gleeble[®] experiments and provides relatively accurate stress measurements. However, there may be significant temperature errors due to thermal resistance at the interface. Third, the thermocouple is physically fixed. The positive and negative electrodes of the thermocouple are welded together and then radially wrapped around the sample. The casing is then tightened around the thermocouple, and an external force is applied to tighten the thermocouple on the sample. This arrangement can be seen in Fig. 1. In comparison with the metal mesh method, this approach utilizes an external tension application as a physical means to establish close contact between the thermocouple and sample, thereby ensuring the integrity of both.

The present section discussed the concepts and challenges of high-temperature tensile testing along with their corresponding solutions. Although tensile testing at elevated temperatures allows for the measurement of the mechanical property limits of alloys, the presence of friction under such testing conditions can lead to significant errors in determining the alloy’s mechanical parameters, which in turn affects the accurate characterization of thermal fracture behaviour. Furthermore, disparities between dendrite growth observed during actual casting processes and that observed in high-temperature tensile experiments result in substantial errors due to microstructural changes. It must be recognized that this experiment has inherent limitations which cannot be fully mitigated.

2.2 Constrained Solidification Method

The hot tearing-constrained solidification method is based on the principle that hot tearing originates from within the alloy and propagates to the surface of the casting at the end

of the solidification process due to solidification shrinkage stress. The severity of hot tearing can be assessed by visual observation of the length and width of the external cracks. Commonly utilized inspection techniques are the hot tearing ring detection, the flange bar test, the cylindrical bar test, the spherical bar test, the "C" bar test and "U" model test.

2.2.1 Hot Tearing Ring Test

As seen in Fig. 2, the hot tearing ring mould comprises an open mould constructed from a flat plate and an annular cavity. Upon pouring molten metal into the mould, the resulting cast metal ring shrinks around the cylindrical core. As the liquid metal content decreases within the semi-solid alloy, thermal cracks emerge and propagate in the casting. Once these cracks reach the surface of the casting, they spread along the grain boundaries. The severity of hot tearing can be assessed by direct observation and measurement of the length and width of the cracks [22].

The impact of grain refinement on the hot tearing sensitivity of aluminium alloys was investigated in this study based on the traditional detection method of hot cracks in

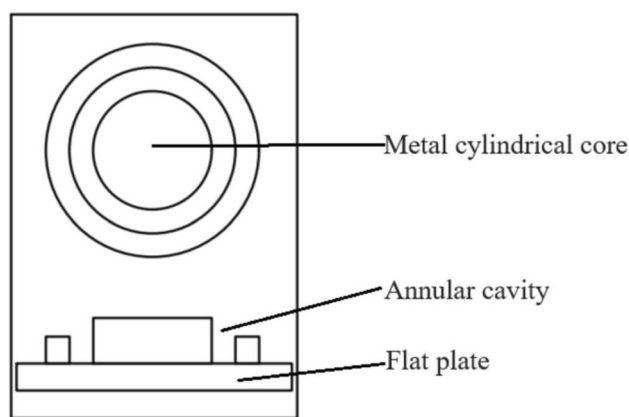
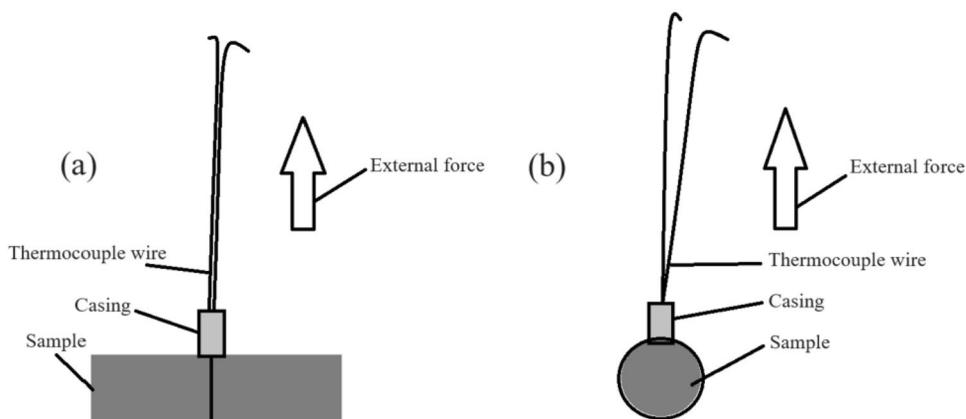


Fig. 2 Schematic diagram of hot tearing ring method mould

Fig. 1 Diagram of connection between thermocouple and specimen



rings. The casting system depicted in Fig. 3 consists of a steel core, a sand box and a gating system with cylindrical gates [23, 24]. After solidification, the alloy's hot tearing sensitivity can be assessed by measuring total crack length of the four rings and calculating the average crack length of each ring. The traditional hot tearing inspection only measures the length of a crack on one ring, taking an average value can partially alleviate the randomness of hot tearing. The use of a closed die helps to avoid external environmental influences on alloy hot tearing. However, in situ observation of cracks during casting solidification is not feasible.

Despite many advantages of the hot crack ring detection method such as simple and convenient operation, low difficulty in mould manufacturing, easy analysis of hot cracks and quick determination of material's relative hot crack sensitivity, it is incapable of detecting hot tearing or micro-cracks within the casting that undergo less shrinkage stress and cannot extend to the surface for observation. The mechanical parameters remain unmeasured, so the extreme stress values of cracks cannot be determined. The random stresses inherent in the solidification process of metals make thermal tearing uncontrollable, thus hindering the study of thermal tearing mechanisms.

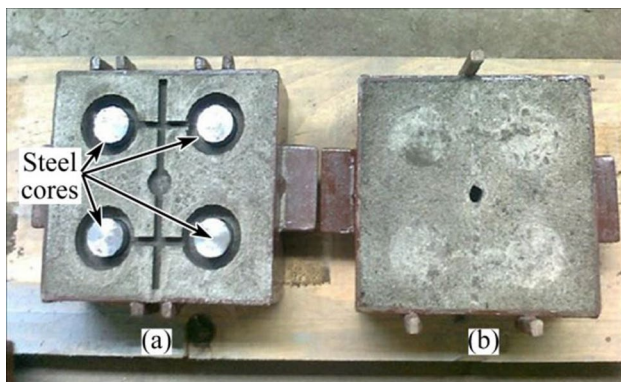
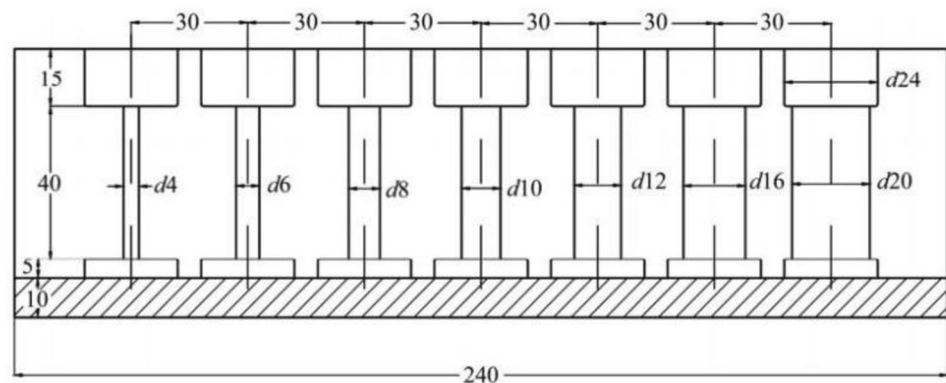


Fig. 3 Hot crack ring detection method closed mould [23]. **a** Casting mould, **b** Cover plate

Fig. 4 Schematic diagram of the critical length test method [25]



2.2.2 Hot Tearing Bar Test

Hot tearing bar detection is the most commonly used macroscopic inspection, which can be classified into two categories: critical diameter testing and critical length testing. Figure 4 illustrates the critical diameter testing method, which consists of multiple bar moulds of the same length but varying diameters. By pouring liquid metal into these moulds, consistent temperature and cooling conditions are maintained across all diameters to ensure that the alloy solidifies in a comparable environment. Thin bars are more susceptible to hot tearing than thick bars due to rapid cooling, high deformation speed, small cross-sectional area and elevated stress levels [25].

The critical length test method is widely recognized as the dominant testing approach [26–29], and the mould used is depicted in Fig. 5. The hot tearing bars with equal diameter are arranged in length. The hot tearing rod is equipped with a spherical mould to induce stress caused by solidification shrinkage. In this method, moulds of the same diameter but different lengths were used and the impact of mould length on hot tearing susceptibility was investigated. This method can also be used in combination with other techniques to study hot tearing sensitivity. For example, the effect of flow on hot tearing sensitivity was studied in combination with a flow device [30], hot tearing sensitivity was studied in combination with tensile property data [31], the effect of grain refinement on hot tearing sensitivity was studied by adding a refining agent [32] or by adding different elements [33, 34].

Akhyar et al. [35] innovatively modified the critical length test method as illustrated in Fig. 6. The hot tearing susceptibility of aluminium alloy was evaluated using the CRCM-horizontal mould method. The dimensions of the mould were $284.4 \times 260.9 \times 30$ mm, and the lengths of the style rods ranged from 51 to 165 mm, separated by an angle of 60° . The sample rod had a diameter of 9.5 mm, while the ball had a diameter of 19 mm. Additionally, the radius of the hot node was 14.5 mm. In contrast to the conventional critical length test method, the experimental design of this

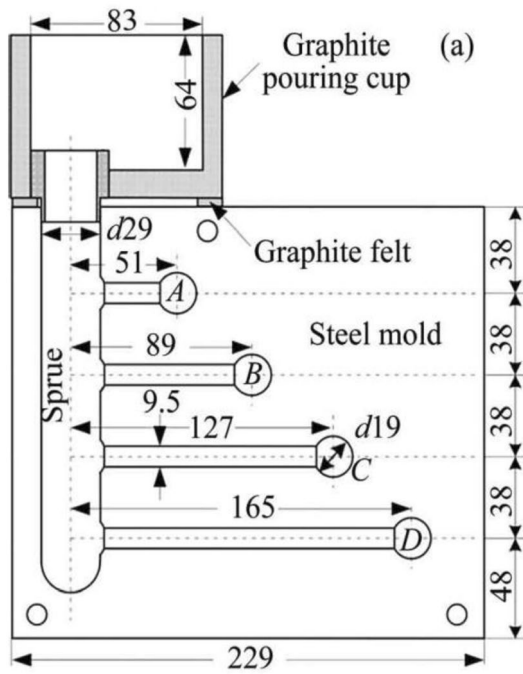


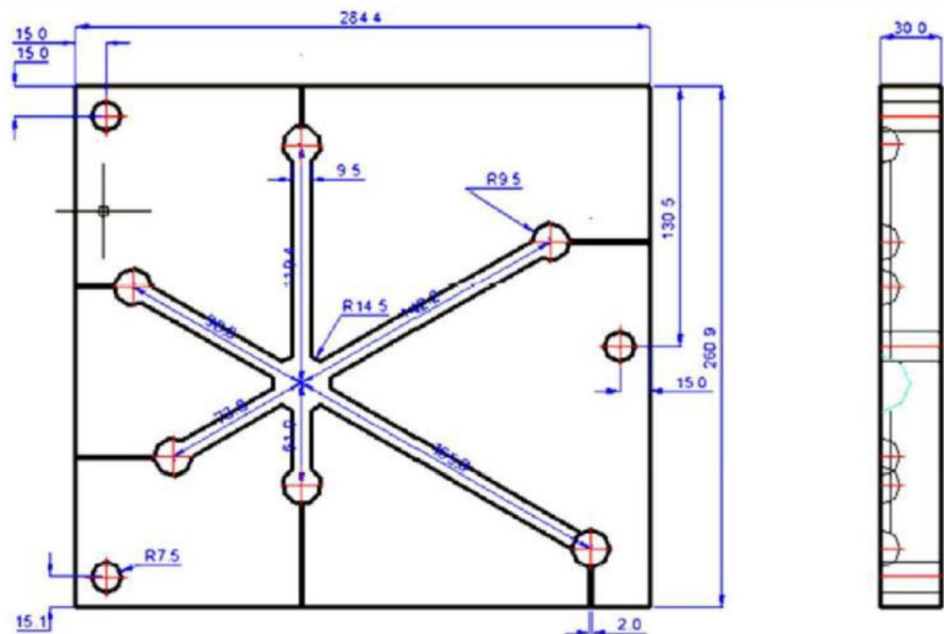
Fig. 5 Mould sketch of critical length test method (mm) [26]

mould involves placing a hot tearing rod on a flat surface and orienting the rods of varying lengths to different directions.

After extensive research and analysis, researchers have identified five levels of hot tearing severity, as illustrated in Fig. 7.

1. There are no cracks or tear marks present on the surface of the rod.

Fig. 6 CRCM- horizontal mould (mm) [35]



2. The presence of cracks is minimal, with microcracks extending to no more than half the circumference of the hot joint.
3. The initial crack has propagated to the entire circumference of the hot joint.
4. The crack is severe, extends throughout the entire circumference of the hot joint and reaches a certain depth.
5. Complete tearing, with complete fracture of the hot section and complete separation of the bar from the casting body.

There are various methods that can be used when it comes to testing the critical length of a material. The advantage of these methods over other techniques is that they produce more precise and accurate results. By applying different levels of stress and strain to a material, researchers can gain valuable insights into the material’s properties and behaviour under different conditions. This information is essential for developing new materials or improving existing ones. In addition, these experimental designs increase the versatility of testing a wide range of materials and provide greater flexibility in testing a variety of materials.

In short, these innovative methods can be considered as an efficient method to test the critical length of a material. Their unique combination of precision and versatility will surely produce valuable data that drives innovative investigations.

2.2.3 Fluid Solidification Test

The influence of fluidity on the development of thermal cracks can be studied by different methods as shown in

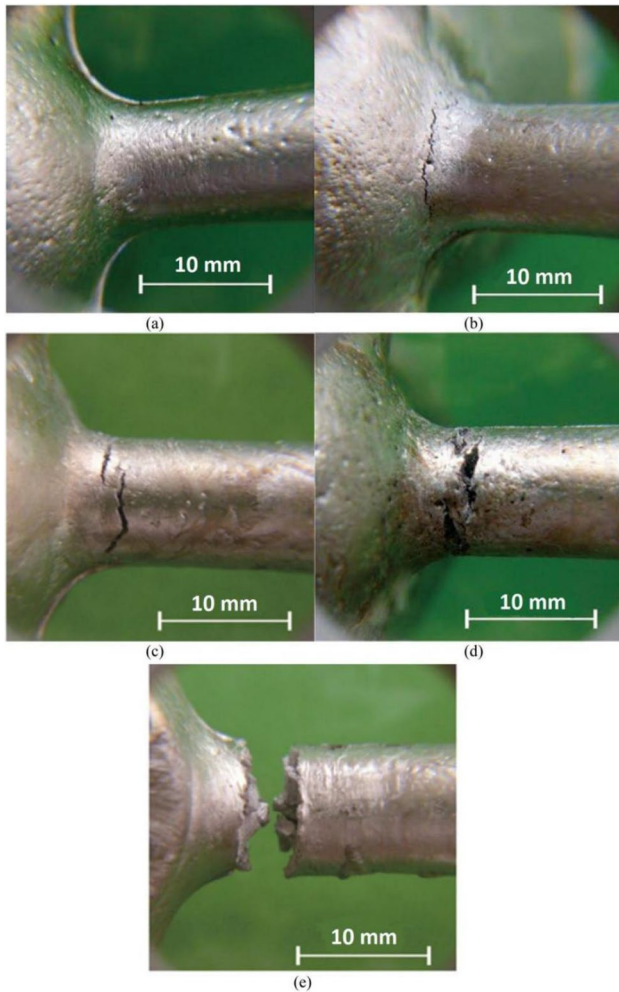
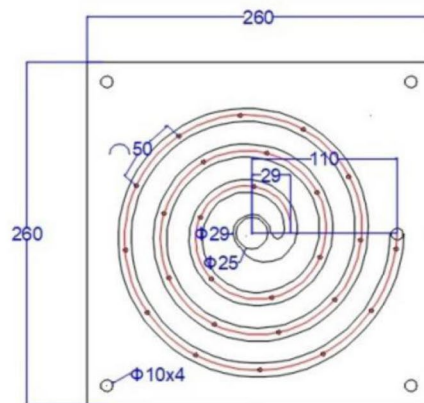
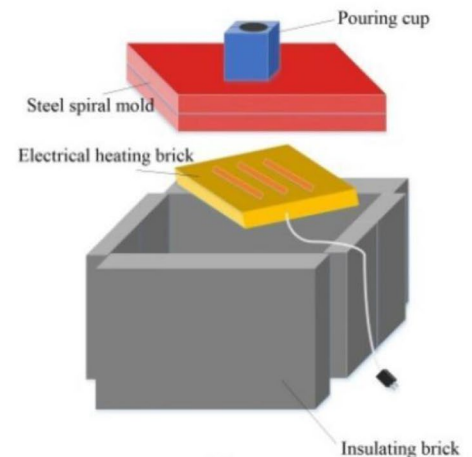


Fig. 7 Schematic diagram of hot tearing severity [35]. **a** no crack, **b** minimal crack, **c** slight crack, **d** serious crack, **e** complete tear

Fig. 8 Flow mould diagram (mm) [36]



(a)



(b)

Fig. 8. The space between the spiral rings is uniformly distributed with a width of 25 mm to ensure consistent and uninterrupted flow of the alloy. A spiral phase jacket with three rings is used to ensure sufficient flow length of the alloy. The greater the flow distance of the alloy in the mould during casting, the better its fluidity and lower the susceptibility to hot cracking [36].

Although constrained solidification and fluid solidification tests allow direct observation of alloy cracking, they can only offer insight into the extent of damage incurred, while the mechanical and temperature parameters associated with hot tearing remain un-inspected. Furthermore, the constrained solidification method solely depicts the final result and there is no investigation of the state alterations in the semi-solid zone during hot tearing formation process. Therefore, it is necessary to develop a method to characterize the stress state of the semi-solid region during alloy solidification. As a result, solidification tensile testing has received increasing attention from researchers.

2.3 Solidification Tensile Test

The solidification tensile test is currently the primary experimental approach for investigating hot tearing of alloys, and most finite element simulation data acquisition relies on this method. The purpose of this method is to replicate the state of alloy during the actual casting process, to observe the hot tearing phenomena, and to study the crack initiation and propagation mechanisms [37]. The solidification tensile test is mainly applied in investigations on the thermal tearing behaviour of alloys from a mechanical perspective based on the strength theory [38–41].

Eskin [42] developed a T-mould in 2002, and after incorporating mechanical sensors, temperature sensors, and data acquisition devices to enhance the system's functionality, they established a sophisticated experimental setup as shown

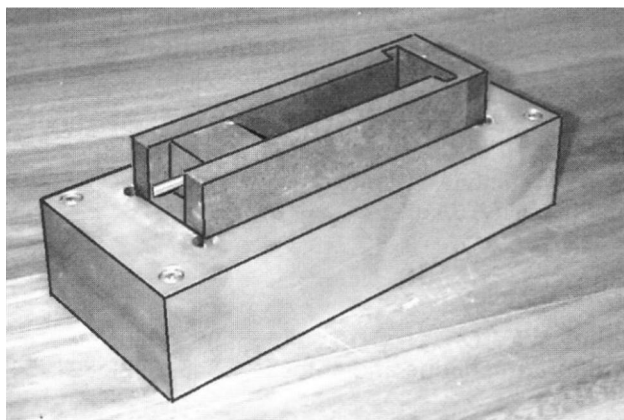


Fig. 9 Diagram of T-mould for Solidification tensile test [42]

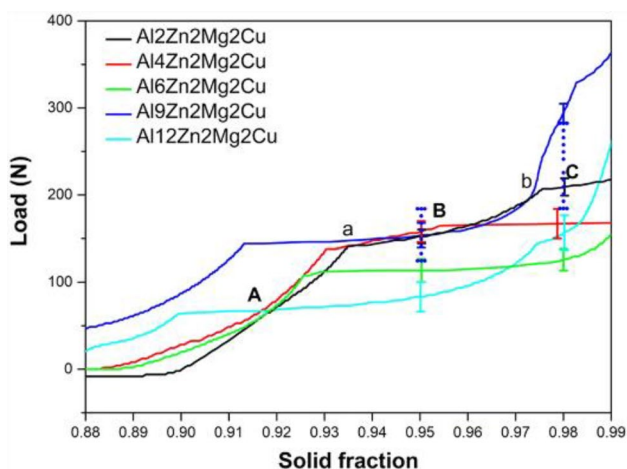


Fig. 10 Diagram of tensile stress with different solid fractions [43]

in Fig. 9. The mould consisted of a T-shaped graphite mould with a graphite block, a bronze base equipped with water cooling, and tension sensors and linear contraction sensors mounted on the device. Temperature variations during metal solidification were measured using a K-type thermocouple.

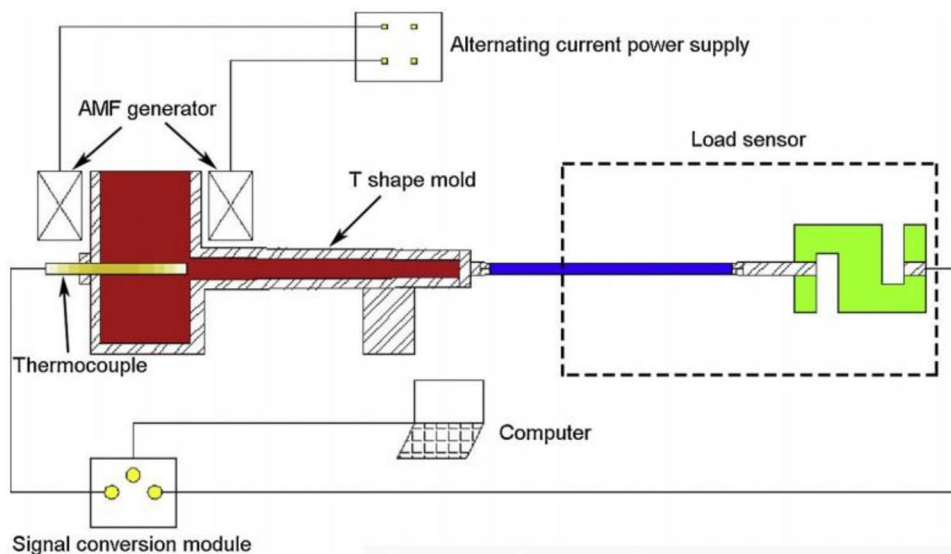
The measured tensile load is shown in Fig. 10. When the solidification stress is equal to or greater than the tensile strength of the dendrite, the specimen fractures and is unstressed. At this stage, the stress caused by solidification shrinkage stabilizes or even decreases, which is negatively correlated with the tendency of the alloy to tear thermally. Therefore, measuring various samples and comparing their solidification shrinkage stress levels can help determine the hot tearing susceptibility of an alloy [43–45].

Another T-mould is illustrated in Fig. 11 [46]. A vertically oriented T-mould was used to measure the solidification shrinkage stress of the alloy utilizing a data acquisition device. The location of crack initiation is determined by the severe tendency to tear at the hot joint, which is identical to the results of the hot tearing bar test. The advantage of this approach lies in its ability to concentrate stress and increase susceptibility to cracking. Using this mould, Xudong Du et al. investigated the influence of rare earth elements addition on hot tearing sensitivity of magnesium alloys [47].

A rod mould is illustrated in Fig. 12, which restricts the hot tear location to the middle region of casting to afford easy identification of initiation point and expansion path of hot tearing. However, as the ends are unconstrained, bolts are required to limit the shrinkage behaviour of the alloy [45, 48].

The dog bone mould shown in Fig. 13 functions in the same way as the rod mould in that it induces hot tearing at the centre of casting, but unlike the rod mould, the dog bone mould has T-shaped ends instead of bolted ends to prevent release of solidification shrinkage stress [49–51].

Fig. 11 Schematic diagram of vertical T-mould [46]



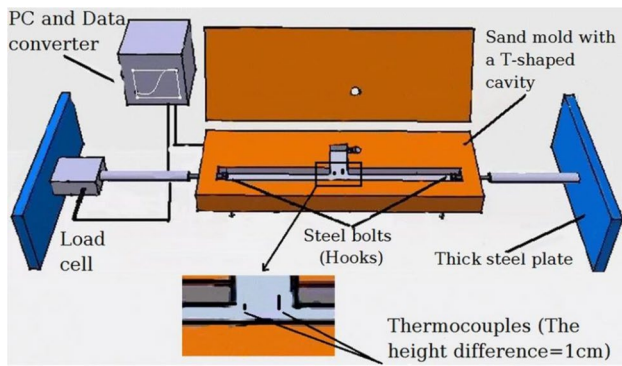


Fig. 12 Schematic diagram of rod mould [48]

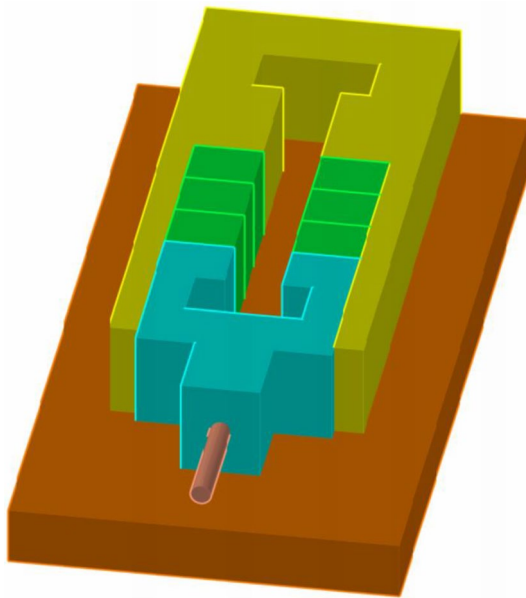
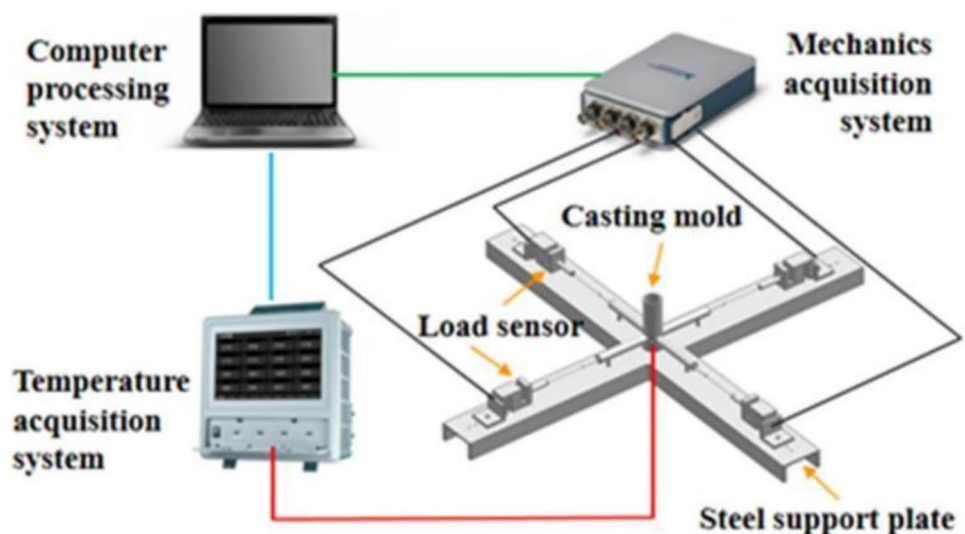


Fig. 13 Schematic diagram of a dog bone mould

Fig. 14 Schematic diagram of composite mould for hot tearing solidification experiment [52]



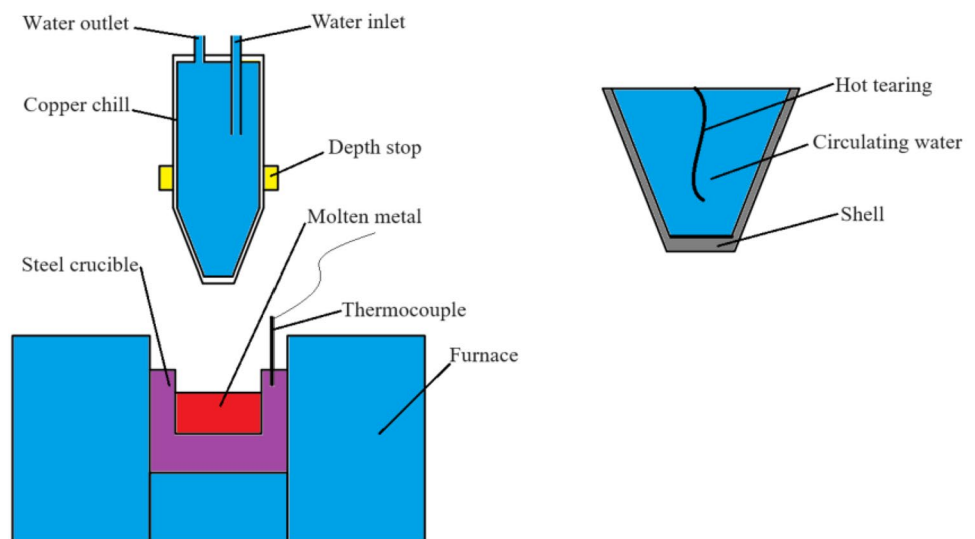
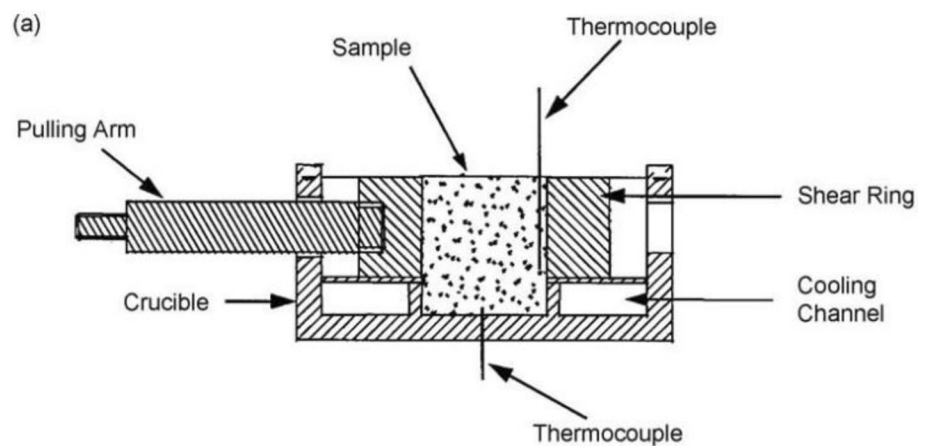
2.4 Multi-channel Hot Tearing Experimental Apparatus

The composite mould illustrated in Fig. 14 employs a multi-channel casting system with thermocouples located at the bottom of the runners and tension sensors to simultaneously capture the solidification shrinkage stress levels of four cylindrical samples, generating a real-time correlation diagram of stress, strain and temperature (solid fraction). Four cylindrical samples with varying diameters are cast in different directions, and the gate was positioned above the intersection of the cylindrical samples. This approach avoids experimental errors that arise from the inability to ensure identical conditions in multiple casting experiments. Moreover, it facilitates the assessment of crack severity in samples with varying diameters and lengths, thereby utilizing the mechanical data to investigate the mechanism of hot tearing generation [52].

2.5 Research Methods of Hot Tearing in Non-traditional Casting Moulds

Warrington D et al. developed an immersive “cold finger” mould to study hot tearing in alloy shells during DC casting as shown in Fig. 15. A water-cooled conical copper cooler was inserted into the thermostatic liquid metal to a specific depth, held for a predetermined duration, and then withdrawn. The length of hot tearing on the shell can be measured to indicate the alloy’s susceptibility to hot tearing [53, 54].

Sumitomo et al. designed a hot shear experiment as shown in Fig. 16 [55]. The molten alloy was initially poured into a central cylindrical mould, and after the liquid metal had cooled to the desired testing temperature, a shear ring was pulled to generate. Subsequently, cooling water was

Fig. 15 Schematic diagram of the “cold finger” mould**Fig. 16** Schematic diagram of hot shear experiment [55]

rapidly introduced into the cooling channel beneath the mould to promote quick solidification of the alloy, while a force-measuring device was used to record the torque of the alloy over time. As the alloy is subjected to tearing and cracking, the torque curve tends to stabilize or even decrease, and the torque value equals the tensile strength of the alloy. When molten metal adheres to a cylindrical mould for dendrite growth, the dendrites grow cylindrically in radial direction and perpendicular to the direction of stress. This method resolves the issue of incapability to assess the strength limit of an alloy in semi-solid state and facilitates the measurement of its strength limit under dendritic relative displacement.

The submerged split-chill tensile (SSCT) test depicted in Fig. 17 was originally proposed by Ackermann et al. as an additional experiment to address the issue of tensile stress in columnar growing in a direction not perpendicular to the direction of the column under conventional Gleeble[®] experimental conditions. The purpose of this experiment was to investigate the mechanical properties of the semi-solid

region. The apparatus comprises a detachable water-cooled shell, a force application mechanism and a water-cooling system. Prior to immersion in liquid metal, the water-cooled shell is stressed by means of the application device to ensure firm attachment. When the shell is submerged in liquid metal, its low surface temperature induces rapid adhesion and formation of columnar crystals, which eventually develop into solid metallic shells with their growth direction perpendicular to the axis of the shell. The device is extracted from the liquid metal, and stress is applied to separate the shell. At this point, the metal shell enclosed by the cylindrical crystals will experience perpendicular tensile stress along its growth direction. When this stress exceeds the limit of the metal shell, it will rupture and form cracks. This method is more suitable for analysing the cracking susceptibility of metal shells before and in the early stages of demoulding due to the rapid cooling rate and thin solid shell during SSCT testing [56, 57].

The modified SSCT experimental setup, shown in Fig. 18, is based on the same principle remains as the original device,

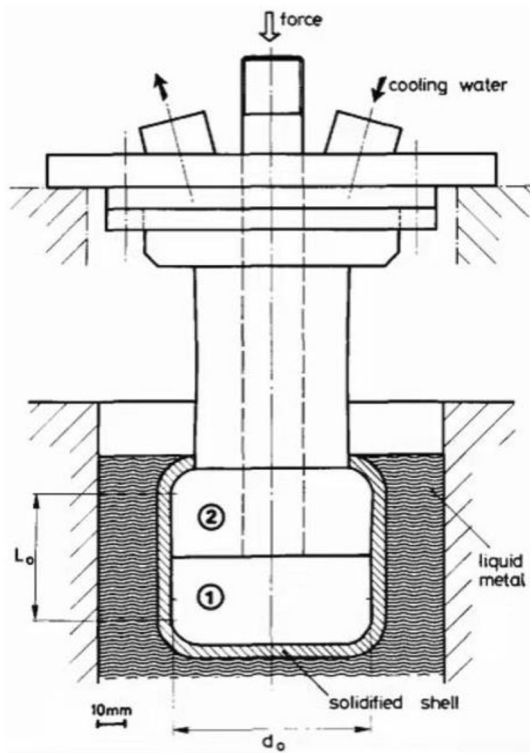


Fig. 17 Schematic diagram of the submerged split-chill tensile (SSCT) test [56]

which employs a detachable water-cooled mould immersed in molten metal and a thicker shell forms on the exterior of the mould; it is then stretched upward and displacement and tension are measured. The exact experimental steps are shown in Fig. 19. A generalized constitutive equation of steel materials during solidification was developed by Pierer et al. using the SSCT device. By analysing stress-force and elongation data of steels with different components under various experimental conditions, it was concluded that the elastic-viscoplastic model yielded the most consistent calculations of the force–elongation curves. Furthermore, this model provided a comprehensive explanation of how variations in strain rate affect the thermal tensile behaviour of steels [58].

Instone et al. [61] developed a CHT stretching device in 2000, as depicted in Fig. 20. The mould was designed with two columnar models: one for recording load and displacement and the other for monitoring hot tearing formation. The ceramic fibre insulation device is positioned at the centre of each bar to fix the solidification direction, ensuring that the solidification front converges at the centre of the bar and forms a substantially uniform temperature field in the cross-sectional direction. Load and displacement measuring devices located at both ends of the left sample monitor and record stress and displacement. This experiment can

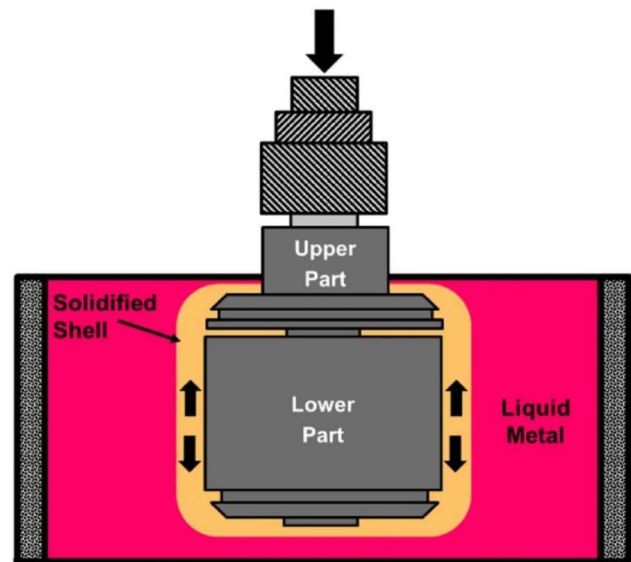


Fig. 18 Diagram of SSCT experimental improvement device [58, 60]

be utilized to investigate the solidification shrinkage stress and hot tearing behaviour of the alloy during solidification under both conditions: without external force [62] and with applied stress [63, 64]. Additionally, cooling devices can be incorporated into the experimental setup to examine crack formation under various cooling boundary conditions.

3 Influence of Various Factors on Hot Tearing Sensitivity

Scholars have devoted considerable attention to the factors affecting hot tearing of alloys, with a specific focus on alloy composition, phase transition factors, dendrite growth characteristics and casting parameters. In general, a range of macroscopic conditions such as casting parameters and changes in alloy composition can alter grain size, dendrite growth pattern, or the formation of second phase, thus affecting the hot tearing susceptibility of the alloy.

3.1 Influence of Alloy Composition on Hot Tearing

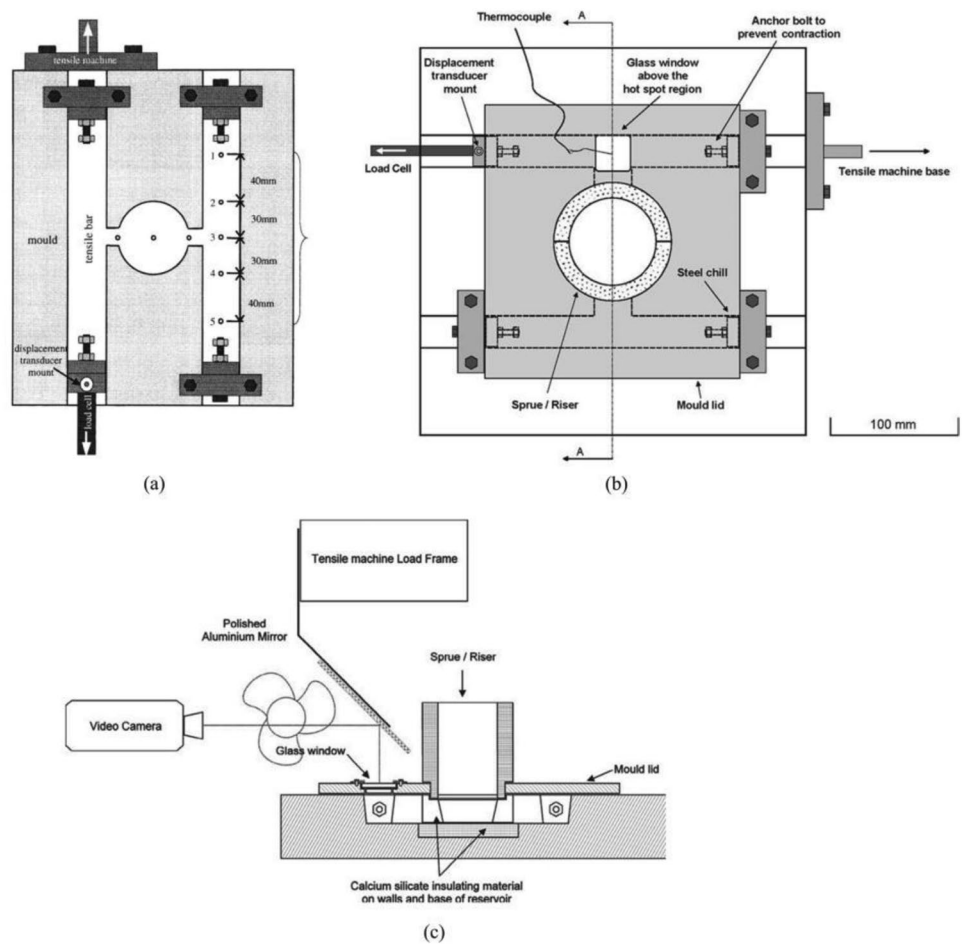
Study on the effect of alloy composition on hot tearing is typically achieved by controlling the content of primary elements in the alloy (such as Zn, Mg, Cu in 7050 alloy), adjusting trace element levels (Fe, Si, etc.), and incorporating intermediate alloys (e.g., AlTiB alloy) or rare earth elements (Ce, La, etc.) to regulate hot tearing susceptibility through grain size manipulation, dendrite growth mode alteration or second phase evolution control.

The finer the grain size, the less susceptible the alloy is to hot tearing. Additionally, a finer grain size results in an

Fig. 19 Procedure of SSCT experiment [59]. **a** The device dips into liquid metal. **b** The device pulls out of the liquid metal. **c** Solidifies the final shape of the housing



Fig. 20 CHT tensile test diagram [61]



extended duration for grains growth to contact with each other, thereby delaying the liquid film feeding. This delay increases the proportion of liquid film feeding relative to the overall solidification time and subsequently decreases the hot tearing sensitivity of the alloy. Furthermore, as the grains become finer, the distribution of solidification shrinkage stress in dendrite grains becomes more uniform, thus decreasing its susceptibility to hot tearing [65].

The second phase has the same crystal structure as the matrix phase of the alloy, which exerts an effective pinning

effect on the grain boundaries during solidification, thereby enhancing the alloy’s strength and effectively reducing its susceptibility to hot tearing [66].

The coherence points of dendrites are commonly investigated. At the initial stage of metal solidification, dendrites are segregated and can move freely. As dendrites continue to grow, their tips constantly collide and interconnect. At this point, the liquid metal can only flow within the solid gap formed by dendrites, which is prone to hot tearing. Therefore, delaying the appearance of coherence points of

dendrites can effectively enhance the feeding efficiency of liquid metal and thus reduce the hot tearing susceptibility of the alloy [67].

Yongqiang Chen et al. [67] investigated the influence of Cu on the hot tearing susceptibility of 7050 alloy by employing a T-mould similar to the one depicted in Fig. 11. The experimental findings demonstrate that the grain size of the alloy decreases with increasing Cu content. The grain size is minimized when Cu content reaches 2%, with optimal amounts of β -phase (Al_2CuMg) and T-phase ($\text{Al}_2\text{Mg}_3\text{Zn}_3$) present along the grain boundaries.

Maria L. Montero-Sistiaga et al. added elemental Si powder to 7075 alloy powder through laser melting and showed that the alloy's melting temperature was significantly reduced with 4% Si addition [68]. This improvement led to enhanced fluidity and significant refinement of the alloy grains, ultimately reducing its hot tearing sensitivity.

Yuxiang Wang et al. [52] investigated the effect of Ce on the hot tearing susceptibility of Al–Cu–Mg–Y alloy. The setup of multi-channel hot tearing experimental apparatus shown in Fig. 14 was used for the experiment. The results show that the addition of Ce can refine the grain structure of Al–Cu–Mg–Y alloy and reduce its sensitivity to hot tearing. However, excessive Ce content leads to grain coarsening and accumulation of $\text{Al}_8\text{Cu}_4\text{Ce}$ phase at grain boundaries, which in turn hinders the liquid metal reinforcement and increases the alloy's susceptibility to hot tearing. Therefore, the optimal effect is achieved at 1% Ce addition.

Nadella et al. [69] studied the effect of adding refiner on hot tearing and segregation of DC casting 7050 alloy by using stress relief annealing immediately after DC casting. The addition of Al–3Ti–1B intermediate alloy has been found to improve the grain refinement in the alloy under identical casting conditions. It has been observed that incorporating a refiner at low casting speeds promotes healing of cracked parts or significantly reduces hot tearing sensitivity at high casting speeds, thereby preventing the occurrence of hot tearing. However, it should be noted that the intermediate alloy has little impact on macroscopic segregation.

3.2 Influence of Casting Process on Hot Tearing

The casting process has a significant impact on the hot tearing of alloys by varying a range of process parameters, including casting speed, cooling rate and application of alternating magnetic fields. These modifications result in changes of the internal grain size, phase transformation or other alterations that ultimately affect the alloy's strength and solidification contraction stress, which in turn affect the susceptibility of the alloy to hot tearing.

Shimin Li et al. [70] investigated the influence of mould temperature and pouring temperature on the hot tearing behaviour of cast aluminium-copper alloy using the

rod-shaped mould depicted in Fig. 12. Material control experiments were conducted using a modified Al–Cu alloy 206 (M206) in comparison with A356 alloy and confirmed the superior hot tearing resistance of A356 alloy. Under the same casting and mould conditions, no cracking was observed in A356 alloy at various mould temperatures, while serious cracking was evident in M206 alloy. The elevation of mould temperature resulted in a notable reduction in both hot tearing susceptibility and severity of linear shrinkage for M206 alloy due to its slower cooling rate caused by higher mould temperature, which consequently decelerated the development of solidification shrinkage stress within the alloy. In contrast, lower mould temperatures increased the temperature gradient and facilitated columnar crystal growth; however, these columnar structures exhibited lower strength along their vertical growth direction, making them susceptible to fracture under stress and thereby promoting the formation of hot tearing within the alloy and increase the hot tearing sensitivity. Furthermore, increasing casting temperature resulted in larger grain size and higher concentration of solidification shrinkage stress, ultimately amplifying hot tearing susceptibility.

Minglong Du et al. [71] investigated the impact of an alternating magnetic field on the hot tearing susceptibility and microstructure of Al–5Cu alloy using a T-mould similar to the one depicted in Fig. 11. The experimental findings revealed that within the range of 0–10 A, as both the magnetic field strength and current increased, vigorous forced convection occurred in the molten metal pool under the action of electromagnetic forces, resulting in dendrite fragmentation and grain refinement. Consequently, the liquid metal feeding channel processed enhanced smoothness while reducing the hot tearing sensitivity of the alloy. However, when subjected to an alternating magnetic field intensity of 15 A, coarse grains were formed due to thermal effect of the electromagnetic field, leading to obstruction of the feeding channel and an increase in hot tearing susceptibility.

The above discussion describes the impact of various factors on the hot tearing sensitivity of alloys. The selection of experimental methodology is crucial when investigating the impact of different factors on hot tearing susceptibility [72]. For instance, conducting a high-temperature tensile test is more suitable for evaluating the solidification shrinkage stress of the alloy, thereby explaining its hot tearing sensitivity from a mechanical perspective. The constrained solidification method is appropriate for macroscopic observation of crack severity in alloys or for modifying their composition to control hot tearing sensitivity. The solidification tensile test comprehensively investigates alloy hot tearing by measuring its stress limit during solidification using mechanical units and examining crack generation under active tensile conditions with a tensile device. Furthermore, how grain refinement affects hot tearing sensitivity can be explored

by studying mould temperature changes and casting temperature variations or by incorporating stirring devices or refiners [73].

4 Trends in Hot Tearing Experiment Research

Experimental approaches for hot tearing research have evolved from simple high-temperature stretching to constrained solidification and then to tensile experiments that simulate the solidification process. However, all three methods employ a single shape or mould for solidification that may deviate from the actual casting process under multi-directional stresses. Therefore, the current testing methods for alloy hot tearing involve a combination of high-temperature tensile tests, constrained solidification and solidification tensile tests, as well as the utilization of numerous sensors to collect experimental data, which ultimately results in a more comprehensive hot tearing testing system.

The high-temperature tensile test has been continuously improved over the past decade, such as the Gleeble[®]-3500 and Gleeble[®]-3800 in the Gleeble[®] Thermal Simulation Experiment series. However, these newer models are based on the same fundamental principles as their predecessors, except for the addition of precision measurement elements. Therefore, even the most basic Gleeble[®]-1500 and Gleeble[®]-2000 tensile testing machines can fully satisfy current experimental requirements. High-temperature tensile testing machines such as the Gleeble[®] series of tensile testing machines still represent the pinnacle of physical simulation worldwide, making the Gleeble[®] tensile test an indispensable method for assessing hot tearing sensitivity in alloys for years to come. However, as simulations continue to advance, the Gleeble[®] test must be adapted to increasingly complex and changing environments.

The hot tearing-constrained solidification method has been favoured by researchers because of its simplicity, ease of implementation and intuitive results, but is unreliable as a primary means of experimentation without data support due to the significant experimental error and subjective conclusions. Currently, hot tearing-constrained solidification studies are less convincing than solidification tensile tests. Therefore, hot tearing-constrained solidification experiments are primarily utilized as supplementary measures for hot tearing assessment, whose results can be integrated with those of the solidification tensile test. In other words, preliminary conclusions are derived from the former test, and these conclusions can be reinforced by data obtained from the latter. The combination of both factors yields a more compelling experimental inference and mitigates inaccuracies.

Solidification tensile testing is currently the most widely used experimental method, of which the results are supported by authoritative data. It can simulate the

real-time process of alloy solidification and hot tearing in casting and is a preferred choice for data acquisition in simulating alloy hot tearing. The future development direction of solidification and tensile experiments is to enhance data collection, adopt more precise testing methodologies, minimize errors and account for the tendency of hot cracking under multi-directional forces, so that the experimental process gets closer to the actual casting production process.

Additionally, we can employ diverse mould shapes, integrate various cooling facilities and adjust casting conditions to investigate the mechanism of hot tearing formation under different circumstances. As previously mentioned, we have the option of utilizing T-shaped moulds, rod moulds or dog bone moulds. Furthermore, by strategically placing a cold iron or controlled cooling device near the mould, we can regulate cooling speed and prevent the formation of hot cracks. Furthermore, by adjusting the casting temperature, pouring speed and mould preheating and cooling speed, diverse testing environments can be created to study the impact of various process parameters on thermal tearing. Taking into account the varying degrees of influence of different factors on alloy hot tearing and the complex conditions present in casting process, it is possible to determine specific values of solidification shrinkage stress or cooling rates that induce hot tearing in alloys. Last but not least, a comprehensive analysis of various data is necessary to investigate the effect of different environments on alloy hot tearing and to evaluate the casting process for effective prevention of thermal cracking.

Acknowledgements This work was financially supported by Basic research expenses of universities directly under the Inner Mongolia (No. JY20220260). Inner Mongolia Autonomous Region Major Science and Technology project (No. 2020ZD0024). Program for Innovative Research Team in Universities of Inner Mongolia Autonomous Region (No. NMGIRT2211), Inner Mongolia University of Technology Key Discipline Team Project of Materials Science (No. ZD202012).

Declarations

Conflict of interest We would like to acknowledge that authors don't have any conflicts of interest.

References

1. Bishop H F, Ackerlind C G, and Pellini W S, *AFS Trans* **60** (1952) 818.
2. Bishop H F, Ackerlind C G, and Pellini W S, *AFS Trans* **65** (1957) 247.
3. Pellini W S, *Foundary* **80** (1952) 125.
4. Campbell J, *Castings*, 2nd edition, Elsevier, (2003), eBook ISBN: 9780080488448
5. Clyne T W, Wolf M, and Kurz W, *Metall Trans* **13B** (1982) 259.

6. Beeley P, *Foundry Technology*, (2001) p 100
7. Li Y, Li H, Katgerman L, Qiang D, Zhang J, and Zhuang L, *Prog Mater Sci* **117** (2021) 100741. <https://doi.org/10.1016/j.pmatsci.2020.100741>
8. Yanru L, Bartlett L N, and O'Malley R J, *Int J Metalcast* **16** (2022) 45. <https://doi.org/10.1007/s40962-021-00599-3>
9. Haafte W M, Kool W H, and Katgerman L, *J Mater Eng Perform* **11** (2002) 537. <https://doi.org/10.4028/www.scientific.net/MSF.217-222.1505>
10. Chu M G, and Granger D A, *Mater Sci Forum* **217–222** (1996) 1505. <https://doi.org/10.4028/www.scientific.net/MSF.217-222.1505>
11. Magnin B, Maenner L, Katgerman L, and Engler S, *Mater Sci Forum* **217–222** (1996) 1209. <https://doi.org/10.4028/www.scientific.net/MSF.217-222.1209>
12. Subroto T, Miroux A, Eskin D G, and Katgerman L, *Mater Sci Eng* **679** (2017) 28. <https://doi.org/10.1016/j.msea.2016.10.021>
13. Giraud E, Suery M, and Coret M, *Metall Mater Trans A* **41** (2010) 2257. <https://doi.org/10.1007/s11661-010-0268-5>
14. Phillion A B, Thompson S, Cockcroft S L, and Wells M A, *Mater Sci Eng A* **497** (2008) 388. <https://doi.org/10.1016/j.msea.2008.07.027>
15. Phillion A B, Cockcroft S L, and Lee P D, *Mater Sci Eng A* **491** (2008) 237. <https://doi.org/10.1016/j.msea.2008.01.078>
16. Han Q, Hassan M I, Saito K, Viswanathan S, and Das S K, *Metall Mater Trans A* **36** (2005) 2073. <https://doi.org/10.1007/s11661-005-0328-4>
17. Subroto T, Miroux A, Eskin D G, Ellingsen K, Marson A, M'Hamdi M, Katgerman L, *13th International Conference on Fracture*, Beijing, China (2013)
18. Bolouri A, Liu K, and Chen X, *Metall Mater Trans A* **47** (2016) 6466. <https://doi.org/10.1007/s11661-016-3744-8>
19. Fabrègue D, Deschamps A, Suéry M, and Poole W J, *Metall Mater Trans A* **37** (2006) 1459. <https://doi.org/10.1007/s11661-006-0090-2>
20. Colley L J, Wells M A, and Maijer D M, *Mater Sci Eng A* **386** (2004) 140. <https://doi.org/10.1016/j.msea.2004.07.019>
21. Bai Q, Li H, Qiang D, Zhang J, and Zhuang L, *Int J Miner Metall Mater* **23** (2016) 949. <https://doi.org/10.1007/s12613-016-1311-3>
22. Lin S, *A Study of Hot Tearing in Wrought Aluminum Alloys*, DEng Thesis, Chicoutimi: University of Quebec (1999), p 187
23. Birru A K, and Benny Karunakar D, *Trans Nonferrous Metals Soc China* **26** (2016) 1783. [https://doi.org/10.1016/S1003-6326\(16\)64291-7](https://doi.org/10.1016/S1003-6326(16)64291-7)
24. Benny Karunakar D, Rai R N, Patra S, and Datta G L, *Int J Adv Manuf Technol* **45** (2009) 851. <https://doi.org/10.1007/s00170-009-2037-4>
25. Bing Z, Shuai L, Kai-le X, Chun X, Zhan-yong W, and Bin-jun W, *Trans Nonferrous Metals Soc China* **30** (2020) 318. [https://doi.org/10.1016/S1003-6326\(20\)65215-3](https://doi.org/10.1016/S1003-6326(20)65215-3)
26. Taghiabadi R, Fayegh A, Pakbin A, Nazari M, and Ghoncheh M H, *Trans Nonferrous Metals Soc China* **28** (2018) 1275. [https://doi.org/10.1016/S1003-6326\(18\)64783-1](https://doi.org/10.1016/S1003-6326(18)64783-1)
27. Sun Y G, Su Y N, Du Z M, Chen L H, and Wang C S, *IOP Conf Ser Mater Sci Eng* (2017). <https://doi.org/10.1088/1757-899X/230/1/012036>
28. Dubey S N, and Ghorieshi J, *Int J Metalcast* **15** (2021) 1412. <https://doi.org/10.1007/s40962-020-00570-8>
29. Liu F, Zhu X, and Ji S, *J Alloys Compd* **821** (2020) 153458. <https://doi.org/10.1016/j.jallcom.2019.153458>
30. Papparattanapong K, Pandee P, Boontein S, and Limmaneevichitr C, *Trans Indian Inst Metals* **71** (2018) 1583. <https://doi.org/10.1007/s12666-018-1293-0>
31. Ganjehfard K, Taghiabadi R, Noghani M T, and Ghoncheh M H, *Int J Miner Metall Mater* **28** (2021) 718. <https://doi.org/10.1007/s12613-020-2039-7>
32. Zhang X, Li D, Zeng L, Wan X, Feng B, and Ren J, *Ceram Int* **46** (2020) 10610. <https://doi.org/10.1016/j.ceramint.2020.01.065>
33. Bo H, Li D, Li Z, Jiangkun X, Wang X, and Zeng X, *Metall Mater Trans A* **52** (2021) 789. <https://doi.org/10.1007/s11661-020-06101-8>
34. Nabawy A M, Samuel A M, Doty H W, and Samuel F H, *Int J Metalcast* **15** (2021) 1362. <https://doi.org/10.1007/s40962-020-00559-3>
35. Akhyar H, Malau V, and Iswanto P T, *Results Phys* **7** (2017) 1030. <https://doi.org/10.1016/j.rinp.2017.02.041>
36. Zou G, Chai Y, Shen Q, Cheng T, and Zhang H, *Int J Metalcast* **16** (2022) 909. <https://doi.org/10.1007/s40962-021-00649-w>
37. Langlais J, and Gruzleski J E, *Mater Sci Forum* **331–337** (2000) 167. <https://doi.org/10.4028/www.scientific.net/MSF.331-337.167>
38. Zhang L, Eskin D G, Lalpoor M, and Katgerman L, *Mater Sci Eng A* **527** (2010) 3264. <https://doi.org/10.1016/j.msea.2010.02.005>
39. Li Y, Gao X, Zhang Z R, Xiao W L, Li H X, Du Q, Katgerman L, Zhang J S, and Zhuang L Z, *Metall Mater Trans A* **48** (2017) 4744. <https://doi.org/10.1007/s11661-017-4251-2>
40. Zhu G, Wang Z, Qiu W, Zhou Y, Zhou L, Wang F, Liu Z, and Mao P, *Int J Metalcast* **14** (2020) 179. <https://doi.org/10.1007/s40962-019-00352-x>
41. Han J Q, Wang J S, Zhang M S, and Niu K M, *Trans Nonferrous Metals Soc China* **30** (2020) 2311. [https://doi.org/10.1016/S1003-6326\(20\)65381-X](https://doi.org/10.1016/S1003-6326(20)65381-X)
42. Eskin D G, Zuidema J, and Katgerman L, *Int J Cast Metals Res* **14** (2002) 217–223. <https://doi.org/10.1080/13640461.2002.11819440>
43. Li Y, Zhang Z R, Zhao Z Y, Li H X, Katgerman L, Zhang J S, and Zhuang L Z, *Metall Mater Trans A* **50** (2019) 3603. <https://doi.org/10.1007/s11661-019-05268-z>
44. Eskin D G, Katgerman L, and Mooney J F, *Metall Mater Trans A* **35** (2004) 1325. <https://doi.org/10.1007/s11661-004-0307-1>
45. Bhiogade D S, Randiwe S M, and Kuthe A M, *Int J Metalcast* **13** (2019) 166. <https://doi.org/10.1007/s40962-018-0246-z>
46. Zhou Y, Mao P, Wang Z, Zhou L, Wang F, and Liu Z, *J Mater Process Technol* **282** (2020) 116679. <https://doi.org/10.1016/j.jmatprotec.2020.116679>
47. Xudong D, Wang F, Wang Z, Zhou L, Liu Z, and Mao P, *J Magn Alloys* **11** (2023) 694–705. <https://doi.org/10.1016/j.jma.2021.05.015>
48. Nasresfahani M R, and Niroumand B, *Int J Metalcast* **14** (2020) 538. <https://doi.org/10.1007/s40962-019-00378-1>
49. Novikov I I, *Goryachelomkost tsvetnykh metallov i splavov (Hot shortness of non-ferrous metals and alloys)*, Nauka, Moscow (1966), p 299.
50. Drezet J-M, Mireux B, Kurtuldu G, Magdysyuk O, and Drakopoulos M, *Metall Mater Trans A* **46** (2015) 4183. <https://doi.org/10.1007/s11661-015-3041-y>
51. Drezet J-M, Mireux B, Szaraz Z, and Pirling T, *Materials* **7** (2014) 1165. <https://doi.org/10.3390/ma7021165>
52. Wang Y, Yue C, Ming S, Yuan X, and Zheng B, *J Mater Eng Perform* **31** (2022) 6349. <https://doi.org/10.1007/s11665-022-06690-y>
53. Warrington D, and McCartney D G, *Cast Metals* **2** (1989) 134. <https://doi.org/10.1080/09534962.1989.11818994>
54. Warrington D, and McCartney D G, *Cast Metals* **3** (1991) 202. <https://doi.org/10.1080/09534962.1990.11819040>
55. Sumitomo T, StJohn D H, and Steinberg T, *Mater Sci Eng: A* **289** (2000) 18. [https://doi.org/10.1016/S0921-5093\(00\)00936-9](https://doi.org/10.1016/S0921-5093(00)00936-9)
56. Ackermann P, Kurz W, and Heinemann W, *Mater Sci Eng* **75** (1985) 79. [https://doi.org/10.1016/0025-5416\(85\)90179-X](https://doi.org/10.1016/0025-5416(85)90179-X)
57. Bernhard C, Hiebler H, and Wolf M M, *ISIJ Int* **36** (1996) 163. https://doi.org/10.2355/isijinternational.36.Suppl_S163
58. Pierer R, Bernhard C, and Chimani C, *BHM Berg- und Hüttenmännische Monatshefte* **150** (2005) 163. <https://doi.org/10.1007/BF03165316>

59. Rowan M, Thomas B G, Pierer R, and Bernhard C, *Metall Mater Trans B* **42** (2011) 837. <https://doi.org/10.1007/s11663-010-9470-5>
60. Lu Y, Bartlett L, O'Malley R, Lekakh S, Buchely M, *AISTech 2020-Proceedings of the Iron & Steel Technology Conference*. <https://www.researchgate.net/publication/343340561>
61. Instone S, St John D, and Grandfield J, *Int J Cast Metals Res* **12** (2000) 441. <https://doi.org/10.1080/13640461.2000.11819381>
62. Viano D, StJohn D, Grandfield J, and Caceres C, *Essential Read Light Metals* **3** (2016) 895. https://doi.org/10.1007/978-3-319-48228-6_112
63. Davidson C, Viano D, Lu L, and StJohn D, *Int J Cast Metals Res* **19** (2006) 59. <https://doi.org/10.1179/136404606225023291>
64. Easton M A, Wang H, Grandfield J, Davidson C J, StJohn D H, Sweet L D, and Couper M J, *Metall Mater Trans A* **43** (2012) 3227. <https://doi.org/10.1007/s11661-012-1132-6>
65. Zhou Z, Liu Z, Wang Y, Liu S, and Tang W, *Mater Res Express* **6** (2019) 016529. <https://doi.org/10.1088/2053-1591/aae542>
66. Ghoncheh M H, and Shabestari S G, *Metall Mater Trans A* **46** (2015) 1287. <https://doi.org/10.1007/s11661-014-2697-z>
67. Chen Y, Liu Z, Liu S, Guo H, Liu J, and Sheng X, *Int J Metalcast* **15** (2021) 130. <https://doi.org/10.1007/s40962-020-00438-x>
68. Montero-Sistiaga M L, Mertens R, Vrancken B, Wang X, Van Hooreweder B, Kruth J-P, and Van Humbeeck J, *J Mater Process Technol* **238** (2016) 437. <https://doi.org/10.1016/j.jmatprotec.2016.08.003>
69. Nadella R, Eskin D, and Katgerman L, *Mater Sci Technol* **19** (2013) 1327. <https://doi.org/10.1179/174328407X236580>
70. Li S, Sadayappan K, and Apelian D, *Metall Mater Trans B* **47** (2016) 2979. <https://doi.org/10.1007/s11663-016-0739-1>
71. Minglong D, Wang F, Xudong D, Wang W, Mao P, Wang Z, Zhou L, and Liu Z, *Int J Metalcast* **17** (2023) 373. <https://doi.org/10.1007/s40962-022-00781-1>
72. Eskin D G, and Katgerman L, *Prog Mater Sci* **49** (2004) 629. [https://doi.org/10.1016/S0079-6425\(03\)00037-9](https://doi.org/10.1016/S0079-6425(03)00037-9)
73. Bai Q L, Li Y, Li H X, Du Q, Zhang J S, and Zhuang L Z, *Metall Mater Trans A* **47** (2016) 4080. <https://doi.org/10.1007/s11661-016-3588-2>

Publisher's Note Springer Nature remains neutral with regard to jurisdictional claims in published maps and institutional affiliations.

Springer Nature or its licensor (e.g. a society or other partner) holds exclusive rights to this article under a publishing agreement with the author(s) or other rightsholder(s); author self-archiving of the accepted manuscript version of this article is solely governed by the terms of such publishing agreement and applicable law.